

# Development of a fast electromagnetic shutter for compressive sensing imaging in scanning transmission electron microscopy

A. Béché,<sup>1, a)</sup> B. Goris,<sup>1</sup> B. Freitag,<sup>2</sup> and J. Verbeeck<sup>1</sup>

<sup>1)</sup>*EMAT, University of Antwerp, Groenenborgerlaan 171, 2020 Antwerp, Belgium*

<sup>2)</sup>*FEI Electron Optics, NL-5600 KA, Eindhoven, The Netherlands*

The concept of compressive sensing was recently proposed to significantly reduce the electron dose in scanning transmission electron microscopy (STEM) while still maintaining the main features in the image. Here, an experimental setup based on an electromagnetic shutter placed in the condenser plane of a STEM is proposed. The shutter blanks the beam following a random pattern while the scanning coils are moving the beam in the usual scan pattern. Experimental images at both medium scale and high resolution are acquired and then reconstructed based on a discrete cosine algorithm. The obtained results confirm the predicted usefulness of compressive sensing in experimental STEM even though some remaining artifacts need to be resolved.

Keywords: Compressive sensing; Scanning transmission electron microscope (STEM); Electromagnetic shutter

## I. INTRODUCTION

One of the most challenging topics in modern transmission electron microscopy (TEM) is to perform experiments on soft or beam sensitive materials as they suffer from irradiation damage that can range from structural modification to the complete destruction of the sample. Such sample modifications are even more problematic when 3D or/and analytical characterizations are involved. In order to overcome this issue, a wide range of different approaches are being tested in the TEM community like reduction of the kinetic energy of the fast electrons<sup>1-3</sup>, improving the detection efficiency of cameras<sup>4-7</sup>, time resolved approaches<sup>8-10</sup> and many more. Relatively recently, the concept of compressive sensing was proposed to significantly reduce the electron dose while maintaining all the important features in a TEM or Scanning TEM (STEM) image<sup>11-14</sup>. Compressive sensing is based on the assumption that an image contains a significant amount of redundancy and not all pixels in the image are independent. The condition for a proper image reconstruction is that the original image has a sparse representation in a specific basis which can be chosen prior to image reconstruction<sup>15-17</sup>. Therefore the image can be approximated from a small subset of pixels randomly taken from the completely sampled image. Depending on the redundancy, such reconstructed image can be very close to the fully sampled image while considerably reducing the required dose. The process is somewhat comparable to image compression algorithms that try to represent images with less information by exploiting the redundancy present in a typical image.

Over the last few years, some studies have indeed proposed to apply compressive sensing to transmission electron microscopy images using different types of reconstruction algorithms based on Bayesian dictionary learning technique<sup>12</sup>, wavelet frame based<sup>13</sup> or total variation

inpainting<sup>14</sup>. All this work was done on virtually masked images starting from a fully sampled experimental or stored image and applying a digital mask to it, taking out a number of often randomly selected pixels. This indeed shows a great potential for compressive sensing but should be seen as an idealized simulation assuming that experimental random pixel measurements would be possible. Implementing compressive sensing in practice is complicated by the fact that typical scan engines in STEM microscopes are not designed to be driven in a non-regular pattern as would be required. An alternative is to make use of a beam shutter that can switch the electron beam on and off while keeping the conventional regular scanning pattern. In this paper we present an experimental realization of such a beam shutter based on electromagnetic deflection and demonstrate that we obtain experimental compressive sensing in a STEM in both medium and high resolution. By shuttering the beam using a pseudorandom generator, it was possible to acquire images with a limited number of pixels and reconstruct them using the discrete cosine transform. This demonstrates that compressive sensing became an experimentally viable technique in STEM opening up the predicted advantages of the technique for experimental research.

## II. EXPERIMENTAL SETUP

The aim in compressive sensing acquisition is to illuminate only parts of the sample. Scanning imaging modes are especially well suited for this operation as images are acquired in a pixel by pixel way. Mainly two strategies can be followed to achieve compressive sensing in such mode: (i) blanking the beam in between two illuminated pixels or (ii) driving the scanning coils in a specific way to jump from one pixel to a non-adjacent next pixel. Stevens et al.<sup>12</sup> achieved successful acquisitions with the second strategy in a SEM. Doing this in a STEM is more complicated due to the higher beam location precision and scanning speed that are typically required. Although less interesting in terms of total ac-

<sup>a)</sup>Corresponding author: armand.beche@uantwerpen.be



FIG. 1. *C2 electric contact aperture holder mounted with a solenoid.*

quisition speed, the blanking method has the distinctive advantage of a simpler hardware setup and will allow us to test compressive sensing in STEM. In a TEM, the pre-specimen beam blanker is located at the gun level but suffers from relatively slow response time, making it unattractive for the current purpose of blanking the beam during scanning. Our first challenge was then to realize a sufficiently fast beam shutter compatible with a typical microsecond range dwell times in STEM. The most accessible locations in the illumination system of a modern TEM are the condenser aperture holders. In the design of our TEM microscope, an FEI Titan3 equipped with both probe and image Cs correctors and a Gatan Image Filter (GIF), the C1 apertures are located in the high vacuum region of the gun making it improper for fast access and convenient operation. The C2 aperture further down the illuminating system was consequently the best place to place the shutter. The first step was to design a completely new aperture holder with four electrical feedthrough contacts. A picture of the custom built holder is displayed in Figure 1. The four aperture slots are clearly visible together with four electrical contacts. We deflect the electron beam making use of a simple solenoid wrapped around the first condenser aperture. The solenoid produces a quasi-homogeneous magnetic field at the plane of the aperture which deflects the electrons due to the Lorentz force. At the given winding density, it turns out that a current of 250 mA is capable of deflecting a 300 keV focused probe about 350 nm away from the sample area. A selected area (SA) aperture was introduced in the path of the beam too prevent high angle diffraction signal from reaching the detector when the shutter blanks the beam. The solenoid has a series resistance of  $R_s = 0.75\Omega$  a self-inductance of  $L_s = 0.3$  H and an estimated capacitance of 12 pF<sup>18,19</sup>. These parameters set the maximum switching speed which can

be estimated as  $\tau = \sqrt{(L_s C_s)}$  leading maximum estimated switching speeds of 2 ns, much shorter than typical STEM dwell times.

As the beam deflector was successfully implemented, we had to synchronize the STEM scan engine with the beam deflection in order to properly shutter the beam at given pixel positions. An Arduino<sup>20</sup> microcontroller unit linked to a switched current source was used to drive the deflector coil synchronized with the shutter signal of the GIF CCD. The microcontroller was then programmed to open or close the shutter based on a (pseudo) random<sup>21</sup> generator in synchronization with the scan engine. A pixel will be illuminated if the random generator with uniform probability distribution between 1 and 100 draws a number higher than X, with X the average amount of unblanked pixels we want to obtain over the whole scan. Figure 2 displays a schematic of our experimental setup.

In order to correctly reconstruct the acquired sparsely sampled image, the reconstruction algorithm needs to have access to the acquisition mask, namely knowing when the beam was blanked or unblanked. As the storage space on the microcontroller was limited, we used a workaround to obtain the shutter mask by acquiring a zero loss (ZL) EELS map together with the HAADF STEM image. In addition to obtaining the applied shutter mask, this workaround allowed us to check how efficiently the electron was shuttered by studying the intensity of the zero loss peak which should ideally be high

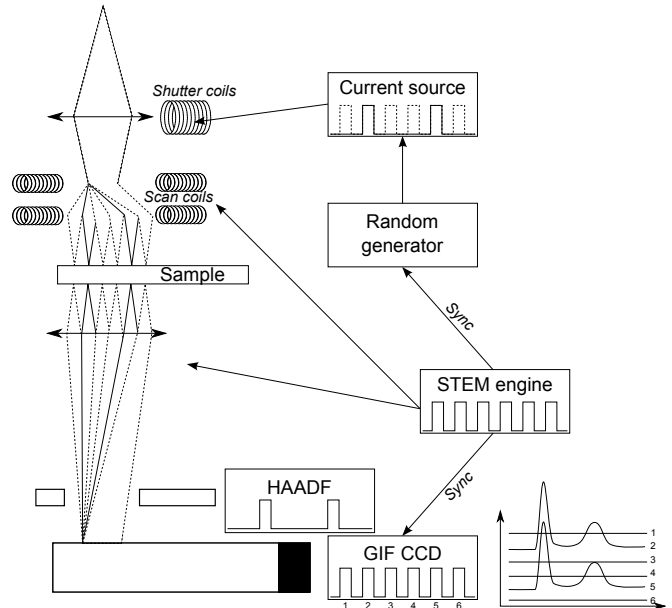


FIG. 2. *Schematic of the compressive sensing acquisition setup. The STEM engine drives the STEM coils and synchronized the GIF CCD and the random generator. Depending on the random number generator, the beam is either blanked (dashed trajectory) or not, leading to the absence or presence of signal on the HAADF detector and zero loss peak in the EELS map.*

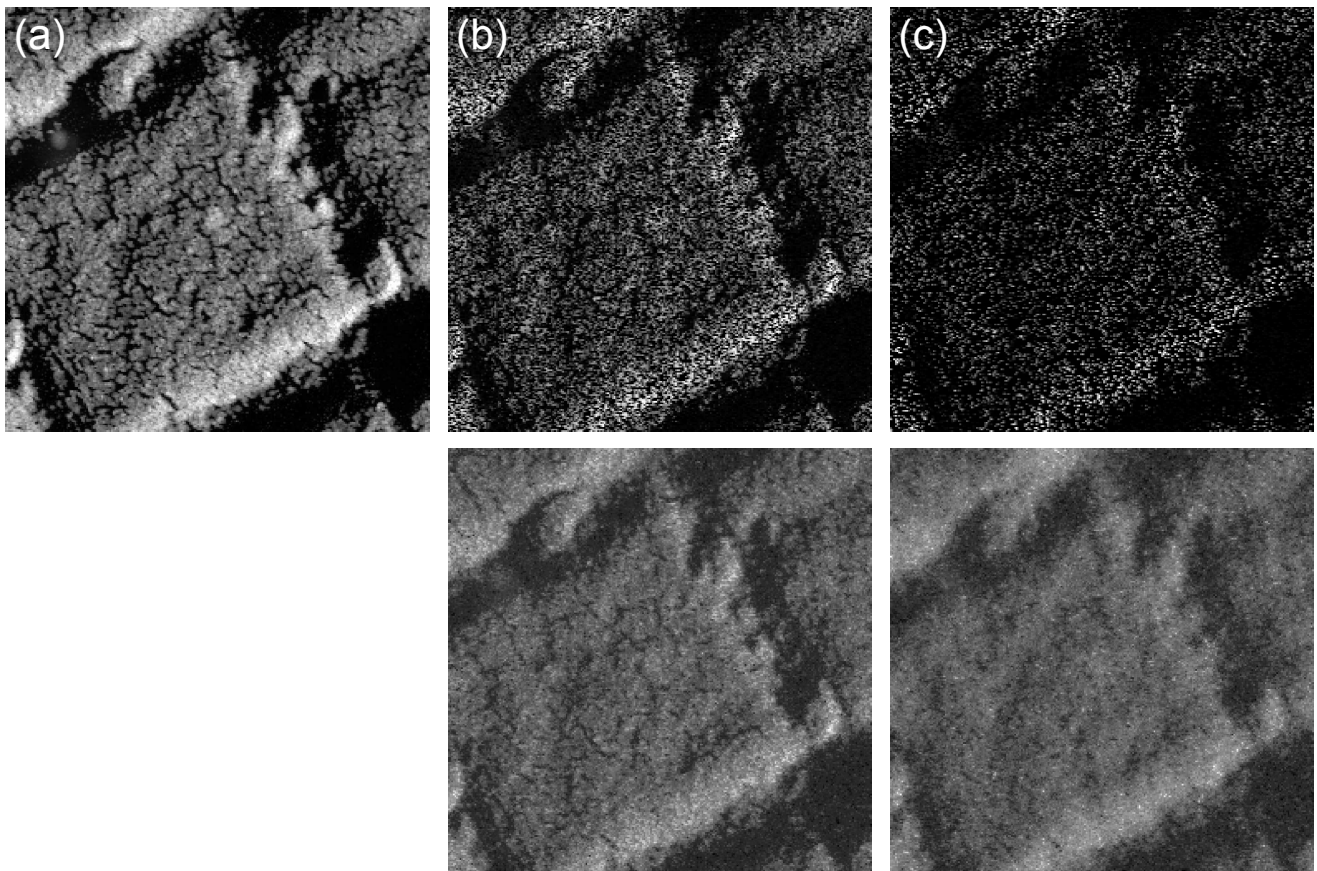


FIG. 3. *Experimental acquisition of STEM images at medium scale using (a) no beam shuttering, (b) 50% beam shuttering and (c) 80% beam shuttering conditions. The reconstructed images based on a discrete cosine algorithm are displayed below the experimental images.*

for unblanked pixels (the sample is electron transparent) and zero for blanked pixels. In order to obtain a ZL peak of sufficient intensity, the single pixel exposure time, for typical High Resolution STEM illumination settings, was set to 0.5 ms. Even though this value is relatively high compared to typical dwell times used in STEM, it nevertheless allows us to prove the setup works and to verify the efficiency of shuttering. In a later stage the described workaround will disappear and the dwell time will be only limited by the maximum speed at which the shutter can be driven which should be well in the microsecond to nanosecond range. In order to reconstruct the images from the subsampled projections, an interpolation is required filling the missing pixels in the images. This interpolation corresponds to solving the following equations:

$$\hat{x} = \operatorname{argmin}_x \|\Phi_x - b\|_{\ell_2} \text{ with } \|\Psi_x\|_{\ell_1} < \lambda \quad (1)$$

Where  $\hat{x}$  corresponds to the reconstructed image,  $b$  equals the measured pixels and  $\Phi$  is a subsampling operator that selects the imaged pixels. The operator  $\Psi$  represents the sparsifying transform that can be chosen prior to the re-

construction and  $\lambda$  is a parameter that can be adjusted according to the sparsity of the image after the sparsifying transform. In this work, a discrete cosine transform is selected which is well suited for images showing a local periodicity such as high resolution STEM projections. The reconstruction is implemented in Matlab using the `spgl1` algorithm<sup>22,23</sup>. More elaborate transforms can easily be implemented but we focused here on the experimental realization of the shutter.

### III. RESULTS

The effect of compressive sensing on STEM image acquisition and reconstruction was investigated using two samples with rather different properties. On the one hand, medium resolution STEM imaging was investigated on a standard gold cross grating sample. This sample has the advantage of presenting a very high density of gold nanoparticles with quite complex agglomerated shapes. On the other hand, HRSTEM was investigated on a complex perovskite oxide sample consisting of an  $\text{NbGaO}_3$  substrate covered with 6 atomic layers of

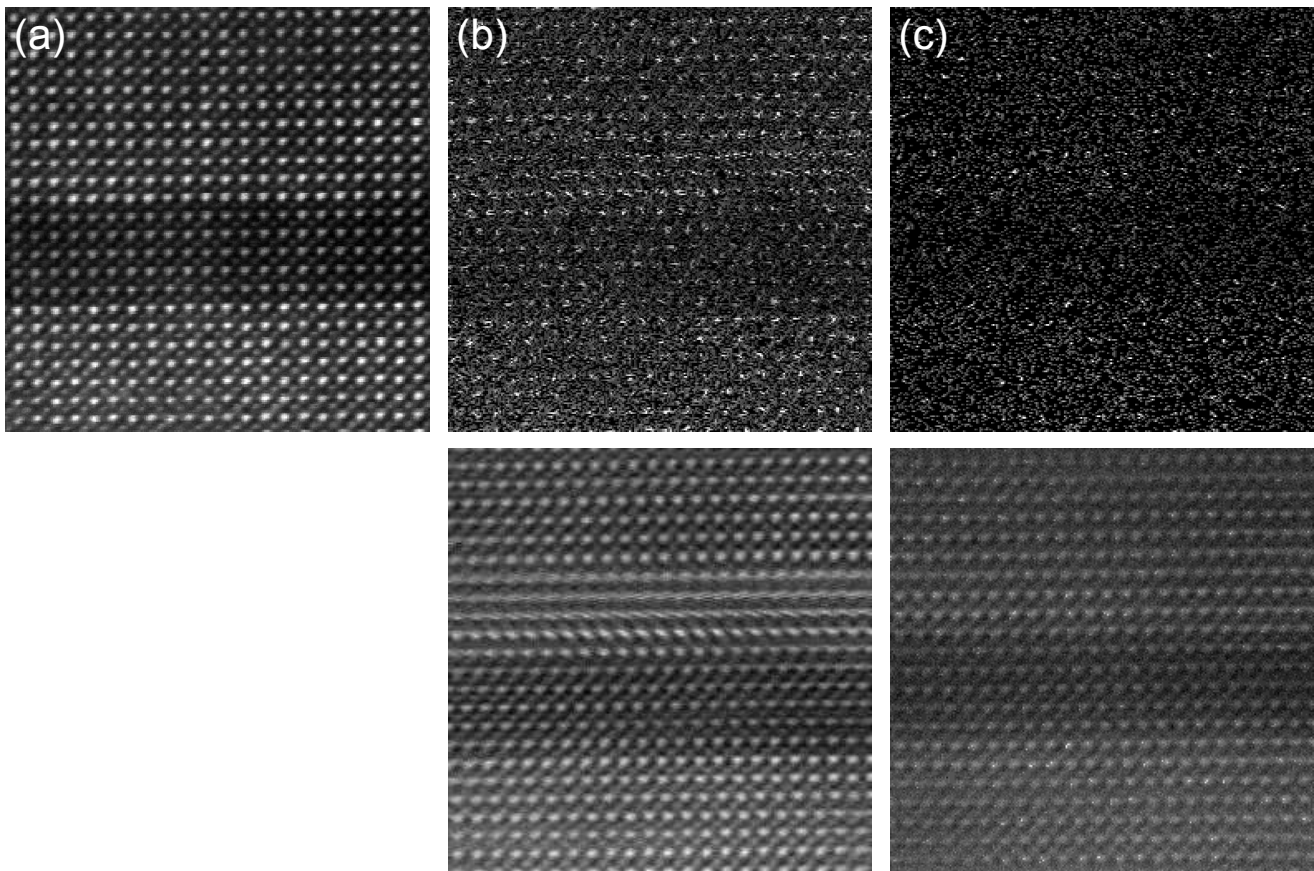


FIG. 4. *Experimental acquisition of STEM images at medium scale using (a) no beam shuttering, (b) 50% beam shuttering and (c) 80% beam shuttering conditions. The reconstructed images based on a discrete cosine algorithm are displayed below the experimental images.*

SrTiO<sub>3</sub> and a 10 nm of LaSrMnO<sub>3</sub><sup>24</sup>. The lattice parameter is well above the theoretical resolution limit of our instrument, thus insuring optimal conditions for the image reconstruction. Both samples also have the advantage of being relatively beam hard allowing for the extra acquisition time needed for the ZL spectrum mapping workaround. One could argue that both samples are rather far from the beam sensitive samples one would expect when discussing compressive sensing, they allow us however to study the feasibility of this new imaging technique without beam damage issues complicating the interpretation of the results. Both samples were imaged with three different acquisition schemes: no shuttering, 50% shuttering and 80% shuttering. The total dose is then effectively reduced respectively by a factor of 2 and 5 in the different cases. The total frame size was set to 256x256 pixels with a dwell time of 0.5 ms in standard HRSTEM illumination conditions, being an acceleration voltage of 300 kV, a convergence angle of 20 mrad with a beam current of 50 pA using a 20  $\mu$ m C2 aperture. The simultaneous ZL EELS map was acquired with a collection angle of 35 mrad using a dispersion of 0.25 eV/pixel and a 5 mm GIF entrance aperture. The experimental

images on the cross grating sample are regrouped in Figure 3 together with their reconstructions based on the discrete cosine algorithm.

For the 50% shuttered case, the main features of the image are retrieved in the reconstructed image, even though the resolution decreased somewhat. The 80% shuttered image reveals a lack of detail and only the larger image features are reconstructed while the finer structural details are lost. Note that in terms of redundancy, the cross grating is probably a very challenging case for compressive sensing for the same reasons that this is an excellent sample to align an electron microscope providing irregular features without favoring certain directions over others.

For the HRSTEM sample displayed in Figure 4, both 50% and 80% shuttering cases are still revealing acceptable high resolution information. The contrast of the lightest atoms tends to significantly decrease in the 80% shuttering case but all atoms remain visible. The presence of the stripes in the middle of the 50% shuttering case are due to some sample instability during the acquisition and do not reflect any issues with the reconstruction algorithm. Because of the longer acquisition times,

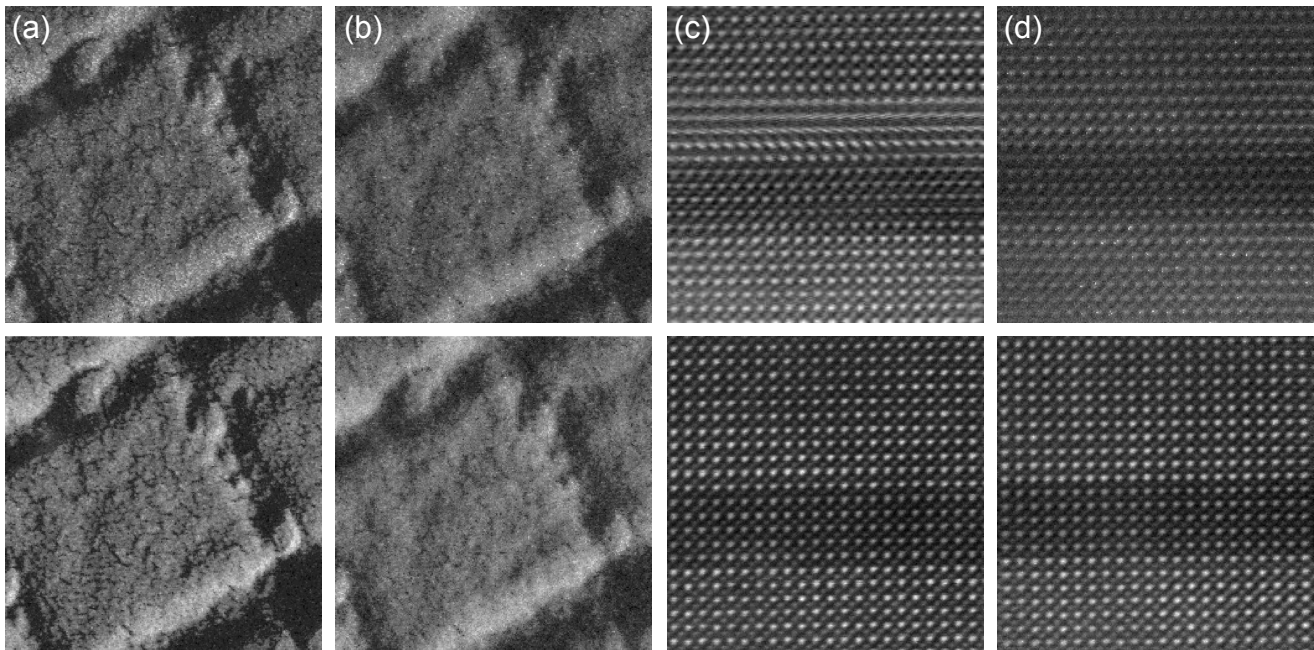


FIG. 5. Comparison between reconstructed images from experiment (top row) and from theory (bottom) row in four cases: (a) cross grating with 50% shuttering time, (b) cross grating with 80% shuttering time, (c) HRSTEM with 50% shuttering time and (d) HRSTEM with 80% shuttering time.

the atomic lattice in Figures 4b and 4c is more distorted by sample drift in comparison to Figure 4a.

#### IV. DISCUSSION

In order to discriminate shutter imperfections from reconstruction issues, we compare the reconstructed images with the reconstructions obtained from a virtually shuttered image obtained by applying a digital mask on the unshuttered experimental HAADF image as was typically done in papers discussing compressive sensing so far<sup>13,14,25</sup>. The results are shown in Figure 5, together with the reconstructed experimental images. In the case of the cross grating sample, simulated and experimental images look very similar, with the small image features being completely lost in the most sparsely sampled case. One can either incriminate the reconstruction algorithm, which may fail to sufficiently exploit the sparsity in the observed object, or it could be that the object itself simply doesn't have enough redundancy to be accurately represented by sparse sampling. For the HRSTEM case, the difference between the virtually shuttered images and the experimental ones is quite significant pointing towards shutter artifacts. For the virtually shuttered images, in both the 50% and 80% shuttered cases, the reconstructions are approaching the fully sampled image quite closely with the only noticeable difference being a slight contrast reduction at sparser sampling. However, the experimentally shuttered image reconstructions suf-

fer from many more artifacts, going from a strong loss of contrast to losing the light atoms all together. These artifacts can have many origins like remaining synchronization and timing issues, sample drift caused by increased exposure times, local sample charging issues affecting probe positioning and possibly others. As sample drift and temporal instabilities of the instrument are related to the total acquisition time, they will disappear when the setup is changed to exploit the full shutter speed as the workaround with the ZL spectral acquisition is removed. Some of the mentioned artifacts could be overcome by using an electrostatic shutter even though this implementation will likely have its own artifacts<sup>26</sup>.

#### V. CONCLUSION

In this paper, we successfully demonstrate the implementation of compressive sensing in a TEM making use of an electromagnetic beam shutter. Using a small solenoid placed in the condenser system of the microscope, the beam can be independently shuttered for every pixel during a STEM image acquisition. The reconstruction of the images from the experimentally obtained sparsely sampled images shows that compressive sensing works significantly better on e.g. high resolution images with much redundancy as compared to more irregular and less redundant images as demonstrated with a cross grating sample. This is entirely expected but has to be kept in mind when estimating the potential reduction in



dose one could obtain from compressive sensing. At the atomic scale, artifacts induced by sample drift significantly alter the result, but can be entirely overcome in the future when lower dwell times are used. The speed of the present setup remains insufficient for realistic use on beam sensitive samples but this limitation is imposed by technological factors which can be overcome in the near future. If these remaining technological challenges are overcome a reduction of dose of at least 5 times can be expected depending on the type and sampling of the object. The implemented solution could offer a cost effective alternative to e.g. a direct electron detection camera or can be combined with it in order to further reduce the dose. Application in 3D tomographic acquisitions seem especially attractive as redundancy between different projections could be exploited. This would be especially important in the case of analytical 3D experiments.

## VI. ACKNOWLEDGEMENTS

A.B, B.G. and J.V. acknowledge funding from the European Research Council under the 7th Framework Program (FP7), ERC Starting Grant No. 278510 VORTEX and No. 335078 COLOURATOM. A.B. and J.V. acknowledge financial support from the European Union under the 7th Framework Program (FP7) under a contract for an Integrated Infrastructure Initiative (Reference No. 312483 ESTEEM2). B.G. acknowledges the Research Foundation Flanders (FWO Vlaanderen) for a postdoctoral research grant. A.B., J.V. acknowledges funding from the GOA project SOLARPAINT and the POC project I13/009 from the University of Antwerp. The Quantem microscope was partially funded by the Hercules Foundation. We thank the Mesa+ laboratory at the University of Twente for the perovskite test sample.

## VII. REFERENCES

- <sup>1</sup>Hh Rose. Criteria and Prospects for Realizing Optimum Electron Microscopes. *Microscopy and Microanalysis*, 13(Supplement S02):134–135, August 2007.
- <sup>2</sup>David A. Muller. Structure and bonding at the atomic scale by scanning transmission electron microscopy. *Nature Materials*, 8(4):263–270, April 2009.
- <sup>3</sup>U. Kaiser, J. Biskupek, J. C. Meyer, J. Leschner, L. Lechner, H. Rose, M. Stger-Pollach, A. N. Khlobystov, P. Hartel, H. Müller, M. Haider, S. Eyhusen, and G. Benner. Transmission electron microscopy at 20 kV for imaging and spectroscopy. *Ultramicroscopy*, 111(8):1239–1246, July 2011.
- <sup>4</sup>Anna-Clare Milazzo, Anchi Cheng, Arne Moeller, Dmitry Lyumkis, Erica Jacovetty, James Polukas, Mark H. Ellisman, Nguyen-Huu Xuong, Bridget Carragher, and Clinton S. Potter. Initial evaluation of a direct detection device detector for single particle cryo-electron microscopy. *Journal of Structural Biology*, 176(3):404–408, December 2011.
- <sup>5</sup>Benjamin E. Bammes, Ryan H. Rochat, Joanita Jakana, Dong-Hua Chen, and Wah Chiu. Direct electron detection yields cryo-EM reconstructions at resolutions beyond 3/4 Nyquist frequency. *Journal of Structural Biology*, 177(3):589–601, March 2012.
- <sup>6</sup>Xueming Li, Paul Mooney, Shawn Zheng, Christopher R. Booth, Michael B. Braumfeld, Sander Gubbens, David A. Agard, and Yifan Cheng. Electron counting and beam-induced motion correction enable near-atomic-resolution single-particle cryo-EM. *Nature Methods*, 10(6):584–590, June 2013.
- <sup>7</sup>G. McMullan, A. R. Faruqi, D. Clare, and R. Henderson. Comparison of optimal performance at 300 keV of three direct electron detectors for use in low dose electron microscopy. *Ultramicroscopy*, 147:156–163, December 2014.
- <sup>8</sup>T. LaGrange, M. R. Armstrong, K. Boyden, C. G. Brown, G. H. Campbell, J. D. Colvin, W. J. DeHope, A. M. Frank, D. J. Gibson, F. V. Hartemann, J. S. Kim, W. E. King, B. J. Pyke, B. W. Reed, M. D. Shirk, R. M. Shuttlesworth, B. C. Stuart, B. R. Torralva, and N. D. Browning. Single-shot dynamic transmission electron microscopy. *Applied Physics Letters*, 89(4):044105, July 2006.
- <sup>9</sup>M. Aidelsburger, F. O. Kirchner, F. Krausz, and P. Baum. Single-electron pulses for ultrafast diffraction. *Proceedings of the National Academy of Sciences*, 107(46):19714–19719, November 2010.
- <sup>10</sup>Philip E. Batson. Unlocking the time resolved nature of electron microscopy. *Proceedings of the National Academy of Sciences*, 108(8):3099–3100, February 2011.
- <sup>11</sup>Peter Binev, Wolfgang Dahmen, Ronald DeVore, Philipp Lamby, Daniel Savu, and Robert Sharpley. Compressed Sensing and Electron Microscopy. In Thomas Vogt, Wolfgang Dahmen, and Peter Binev, editors, *Modeling Nanoscale Imaging in Electron Microscopy*, Nanostructure Science and Technology, pages 73–126. Springer US, 2012.
- <sup>12</sup>Andrew Stevens, Hao Yang, Lawrence Carin, Ilke Arslan, and Nigel D. Browning. The potential for Bayesian compressive sensing to significantly reduce electron dose in high-resolution STEM images. *Microscopy*, 63(1):41–51, January 2014.
- <sup>13</sup>M. Li, Z. Fan, H. Ji, and Z. Shen. Wavelet Frame Based Algorithm for 3d Reconstruction in Electron Microscopy. *SIAM Journal on Scientific Computing*, 36(1):B45–B69, January 2014.
- <sup>14</sup>Zineb Saghi, Martin Benning, Rowan Leary, Manuel Macias-Montero, Ana Borrás, and Paul A. Midgley. Reduced-dose and high-speed acquisition strategies for multi-dimensional electron microscopy. *Advanced Structural and Chemical Imaging*, 1(1):1–10, May 2015.
- <sup>15</sup>Emmanuel J. Cands, Justin K. Romberg, and Terence Tao. Stable signal recovery from incomplete and inaccurate measurements. *Communications on Pure and Applied Mathematics*, 59(8):1207–1223, August 2006.
- <sup>16</sup>D.L. Donoho. Compressed sensing. *IEEE Transactions on Information Theory*, 52(4):1289–1306, April 2006.
- <sup>17</sup>E.J. Candes and M.B. Wakin. An Introduction To Compressive Sampling. *IEEE Signal Processing Magazine*, 25(2):21–30, March 2008.
- <sup>18</sup>R. G. Medhurst. HF resistance and self capacitance of single layer solenoids Part1. *Wireless Engineering*, 24:35–43, February 1947.
- <sup>19</sup>R. G. Medhurst. HF resistance and self capacitance of single layer solenoids Part2. *Wireless Engineering*, 24:80–92, March 1947.
- <sup>20</sup>Arduino - Home.
- <sup>21</sup>S. K. Park and K. W. Miller. Random Number Generators: Good Ones Are Hard to Find. *Commun. ACM*, 31(10):1192–1201, October 1988.
- <sup>22</sup>E. van den Berg and M. Friedlander. Probing the Pareto Frontier for Basis Pursuit Solutions. *SIAM Journal on Scientific Computing*, 31(2):890–912, November 2008.
- <sup>23</sup>SPGL1: A solver for large-scale sparse reconstruction.
- <sup>24</sup>Z. Liao, M. Huijben, Z. Zhong, N. Gauquelin, S. Macke, R.J. Green, S. Van Aert, J. Verbeeck, S. Van Tendeloo, K. Held, G. A. Sawatzky, G. Koster, and G. Rinjders. Controlled lateral anisotropy in correlated manganite heterostructures by oxygen

octahedral coupling. *Nature Materials*, Submitted, 2015.

<sup>25</sup>Hyrum S. Anderson, Jovana Ilic-Helms, Brandon Rohrer, Jason Wheeler, and Kurt Larson. Sparse imaging for fast electron microscopy. volume 8657, pages 86570C–86570C–12, 2013.

<sup>26</sup>Quentin Ramasse. Private Discussion. 2015.